

Article

Water-to-Cement Ratio of Magnesium Oxychloride Cement Foam Concrete with Caustic Dolomite Powder

Weixin Zheng ^{1,2,*}, Xueying Xiao ^{1,2}, Jing Wen ^{1,2}, Chenggong Chang ^{1,2}, Shengxia An ^{3,4} and Jingmei Dong ^{1,2,*}

¹ Key Laboratory of Comprehensive and Highly Efficient Utilization of Salt Lake Resources, Qinghai Institute of Salt Lakes, Chinese Academy of Sciences, Xining 810008, China; xiaoxy@isl.ac.cn (X.X.); wj580420@isl.ac.cn (J.W.); ccg168@isl.ac.cn (C.C.)

² Key Laboratory of Salt Lake Resources Chemistry of Qinghai Province, Xining 810008, China

³ Qinghai Building and Materials Research Co., Ltd., Xining 810008, China; 18297211979@163.com

⁴ The Key Lab of Plateau Building and Eco-Community, Xining 810008, China

* Correspondence: zhengweixin@isl.ac.cn (W.Z.); dongda839@isl.ac.cn (J.D.)

Abstract: Magnesium oxychloride cement (MOC) foam concrete (MOCFC) is an air-hardening cementing material formed by mixing magnesium chloride solution (MgCl₂) and light-burned magnesia (i.e., active MgO). In application, adding caustic dolomite powder into light-burned magnesite powder can reduce the MOCFC production cost. The brine content of MOC changes with the incorporation of caustic dolomite powder. This study investigated the relationship between the mass percent concentration and the Baumé degree of a magnesium chloride solution after bischofite (MgCl₂·6H₂O) from a salt lake was dissolved in water. The proportional relationship between the amount of water in brine and bischofite, and the functional formula for the water-to-cement ratio (W/C) of MOC mixed with caustic dolomite powder were deduced. The functional relationship was verified as feasible for preparing MOC through the experiment.



Citation: Zheng, W.; Xiao, X.; Wen, J.; Chang, C.; An, S.; Dong, J.

Water-to-Cement Ratio of Magnesium Oxychloride Cement Foam Concrete with Caustic Dolomite Powder.

Sustainability **2021**, *13*, 2429. <https://doi.org/10.3390/su13052429>

Academic Editor: José Ignacio Alvarez

Received: 27 January 2021

Accepted: 19 February 2021

Published: 24 February 2021

Publisher's Note: MDPI stays neutral with regard to jurisdictional claims in published maps and institutional affiliations.

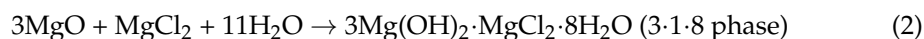
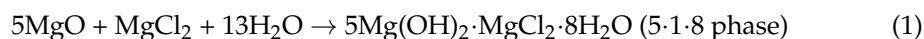


Copyright: © 2021 by the authors. Licensee MDPI, Basel, Switzerland. This article is an open access article distributed under the terms and conditions of the Creative Commons Attribution (CC BY) license (<https://creativecommons.org/licenses/by/4.0/>).

Keywords: magnesium oxychloride cement; bischofite; water-to-cement ratio; caustic dolomite; light-burned magnesite

1. Introduction

Magnesium oxychloride cement (MOC) is formed by mixing magnesium chloride solution (MgCl₂·H₂O) with magnesium oxide powder (MgO) [1,2]. As an air-dried gel material, MOC is widely used in several fields, including construction, transportation and technology [3–6]. At room temperature and pressure, the chemical reactions in the MgO-MgCl₂-H₂O system are the following:



The above equations show that the hydration product of MOC depends on the ratio of the constituents, including the molar ratios of MgO/MgCl₂ and H₂O/MgCl₂ [7]. At present, the MgO raw materials for MOC products are mostly light-burned magnesite (LMP), which can be made from magnesite calcined at 900 to 1050 °C [8,9]. The calcination of MgO allows the preparation of active magnesium oxide (MgO_a), and the degree of crystallization of MgO_a has a strong impact on the hydration reactions in MOC, determining the hydration products and its deformation and strength characteristics. With the continuous growth of the world's requirements for magnesite and the environmental pressure, the price of LMP remains high. MgO_a can be produced from the calcination of magnesite or dolomite [10,11]. Dolomite resources are widely distributed [12]. The economic cost of producing MOC can be effectively reduced by adding caustic dolomite powder (CDP) to the raw material

of LMP. However, CDP cannot be directly applied to the production of MOC due to the MgO components. Dolomite calcinated at a lower temperature may generate calcination products of MgO with CaCO_3 [13]. The MgO content in dolomite is one-third of that of magnesite; therefore, the mechanical performance of MOC prepared with dolomite raw material is poor [14], especially magnesium oxychloride cement foam concrete (MOCFC) made from porous material [15]. Dolomite has already been tested as a raw material for producing MgO-based cements such as magnesium oxychloride cement [16], magnesium oxysulfate cement [17] and magnesium phosphate cement [13]. However, few studies have been conducted using CDP and LMP as the raw materials to produce MOC material, and only a few scholars have probed the performance of MOC made from mixed materials [18]. The ratio between the mixed raw materials and the liquid phase still needs to be determined, as it is significant for the scale production of MOC.

The current raw bischofite ($\text{MgCl}_2 \cdot 6\text{H}_2\text{O}$) for the MOC product is generally obtained from the byproduct of a potash fertilizer [19]. This is because the large amount of the byproduct bischofite in a salt lake area can substantially reduce the manufacturing cost of MOC. For example, in Qarhan Salt Lake, in Qinghai Province, potash production was about 3.7 million tons of K_2O in 2011 and about 3.9 million tons of K_2O in 2012, corresponding to an annual production of about 29 to 39 million tons of bischofite [20]. Salt Lake areas are enriched with a large quantity of bischofite resources that have not been exploited and utilized, which restricts the balance and sustainable development of local resources [21,22]. However, the impurity mass content of bischofite can be 2% or more; see Table 1. The strength of MOC can be reduced with the introduction of waste [14]. The MgCl_2 used in the laboratory or small amounts of MgCl_2 used to study MOC material are obtained as high-purity raw materials [23,24], and some errors may be involved in practical industrial applications when an impure raw material is used [25]. Due to the number of raw materials, their relationships with concrete performance have a great impact [26,27]. In order to use a large amount of bischofite for the scale production of MOC, it is necessary to find the relationship between the quantities of raw materials used for the scale production of MOC. This is of great significance for the popularization and application of economical MOC and its products in the salt lake regions.

Based on the above hypothesis, firstly, the relationship between the quantities of raw materials used in the preparation of MOC with single LMP and pure magnesium chloride were derived, and a derivation of formula (DF) was obtained. Secondly, the calculation method for the MOC raw material mix ratio was revised and simplified in accordance with the actual parameters of bischofite dissolved in water, and thereby, a modification of formula (MF) was obtained. Finally, according to the MF and the relationship between the amount of water in brine and bischofite, a water-to-cement ratio (W/C) function model when using CDP and LMP as the raw material for MOC simultaneously was derived, and the model was verified for MOCFC.

2. Materials and Methods

2.1. Raw and Processed Materials

The MOC raw materials were mixed with caustic dolomite fines, including the potassium byproduct of bischofite, LMP and CDP. The bischofite was produced in Qarhan Salt Lake of Qinghai province. The chemical composition of the bischofite is presented in Table 1. The LMP was produced in Haicheng of Liaoning province. The CDP was prepared in the laboratory. The dolomite ore was mined from Huzhu County, Qinghai Province, China, and its main components are $\text{CaMg}(\text{CO}_3)_2$, CaCO_3 and SiO_2 . The CDP was obtained by calcining the dolomite ore in a Tunnel kiln at a temperature of 750°C , grinding it and then screening it through a 120-mesh sieve. The main chemical constituents of the LMP and CDP were analyzed via X-ray fluorescence (XRF), and the results are presented in Table 2. According to the hydration method and citric acid method [7], the contents of MgO_a of the LMP and CDP were 63.73% and 18.70%, respectively.

Table 1. Chemical composition of bischofite (wt.%).

Component	MgCl ₂	KCl	NaCl	CaCl ₂	MgSO ₄	Water Insolubles	Crystal Water
Bischofite	46.10	0.38	0.46	0.11	0.09	0.45	52.41

Table 2. Chemical composition of light-burned magnesite (LMP) and caustic dolomite powder (CDP) (wt.%).

Component	MgO	SiO ₂	CaO	Al ₂ O ₃	Fe ₂ O ₃	Loss on Ignition
LMP *	85.96	6.03	1.29	1.28	0.57	4.87
CDP *	20.15	1.46	33.20	0.85	0.47	43.87

* The contents of MgO_a in LMP and CDP were 63.73 and 18.70, respectively.

2.2. Brine Test

The mass percentage concentration (P), density (ρ) and Baumé degree (Ba) of MgCl₂–H₂O were tested by dissolving bischofite in tap water. The ρ and Ba were measured with an electronic densitometer and a Baumé meter, respectively. The test was performed three times at the same ambient temperature (20 °C), and the average value was obtained. The weighed bischofite was first placed in a measuring cylinder (1000 mL) and then slowly added to tap water until the bischofite was completely dissolved, at which point the solution was saturated in each test. Afterward, water was added to the saturated solution at 10 different times, so that the total amount of water added was 100 g. After each addition of water, the solution was stirred with a glass rod for 1 min. After the solution was evenly mixed, the Ba and ρ were measured. The amount of water (free water, m_f) and chlorobalite (m_{Bi}) added to the solution at different stages affected the m_f/m_{Bi} ratio, which in turn influenced Ba and ρ . For example, when $m_f/m_{Bi} = 0.55$, the corresponding Ba and ρ were 31.0 and 1276, respectively. The results are presented in Table 3.

Table 3. Test data of the brine.

m_f/m_{Bi}	Ba (°Be')	P (kg/m ³)	P (%)
0.55	31.0	1276	29.7
0.69	28.0	1256	27.9
0.80	26.5	1239	26.3
0.84	25.5	1224	24.9
1.00	24.2	1212	23.6
0.99	23.0	1201	22.4
1.11	22.0	1191	21.4
1.30	21.0	1182	20.5
1.33	20.0	1167	19.6
1.45	19.5	1165	18.8
1.50	19.0	1158	18.0

m_f/m_{Bi} represents the mass ratio between the tap water and bischofite; P was calculated according to Table 1; $P = (m_{MC} \times 46.10\%) / [m_{H_2O} + m_{MC} \times (100 - 46.10)\%] \times 100\%$; m_{MC} and m_{H_2O} are the masses of MgCl₂ and H₂O in the solution.

2.3. MOCFC Test

In the preparation of the MOCFC samples, first, bischofite was dissolved in water, and MgCl₂–H₂O of 25 °Be' was prepared and was then mixed and stirred evenly with LMP. The foam (made from a commercially available animal protein foaming agent) was added to the MOC slurry, and the mixture was evenly mixed (the ratio of the volume of foam added to the mass of the slurry was 400). The mixture was cast in a 100 × 100 × 100 mm test mold. The specimens were covered with plastic film and cured at room temperature for 24 h. The specimens were then removed from the mold and cured in an environment of 20 ± 3 °C and relative humidity of 50% (air humidity). For the 28-day

matured composites, the micromorphology and mechanical performance were determined. The micromorphology was characterized by scanning electron microscopy (SEM, JSM-5610LV) with gold coating. The mechanical performance was investigated with a universal testing machine (WDW-200Y, loading speed of 0.5 ± 0.05 MPa/s).

3. Results and Discussion

3.1. Derivation of Formula (DF)

The results show that a 5·1·8 phase was present in crosslinked needle- and rod-shaped crystals in the MOC, which endowed it with good mechanical properties [23,24]. When the molar ratio of MgO/MgCl₂ was less than 6, the MgO content in the hydration products increased with an increase in the MgO/MgCl₂ molar ratio, which made the original solution more alkaline and ensured the stability of the MOC phase [7]. It is generally believed that MOC products have excellent properties when the MgO/MgCl₂ molar ratio is 5–10 [28–30]; nonetheless, in one study, the mechanical properties of MOC products were best when the molar ratio was approximately 7 [28,29]. Therefore, most researchers and manufacturers usually take the MgO/MgCl₂ molar ratio as the benchmark parameter of the MOC system ratio in current MOC applications.

Let the MgO/MgCl₂ molar ratio be n ; then

$$\frac{n_{\text{MO}}}{n_{\text{MC}}} = n \quad (4)$$

where n_{MO} and n_{MC} represent the molar masses of MgO and MgCl₂, respectively.

The relationship between the MgO mass (m_{MO}) and n_{MO} and the relationship between the brine mass (m_{Br}) and n_{MC} can be deduced using Equations (5) and (6), respectively; in the equations, a is the amount of MgO_{*a*} in the MgO powder:

$$n_{\text{MO}} = \frac{a m_{\text{MO}}}{40} \quad (5)$$

$$n_{\text{MC}} = \frac{P m_{\text{Br}}}{95} \quad (6)$$

where the molar mass of MgO is 40 g/mol and that of MgCl₂ is 95 g/mol. By substituting Equations (5) and (6) into Equation (4), the relationship between the m_{Br} and m_{MO} can be obtained:

$$\frac{m_{\text{Br}}}{m_{\text{MO}}} = \frac{95 a}{40 n P} = 2.375 \frac{a}{n P} \quad (7)$$

Equations (5)–(7) represent the basic relationships of the MOC raw materials. n is defined by the material designer and is often fixed. Therefore, the performance of MOC is usually determined by a and P , with P obtained through Ba . The relationship between the Ba value of MgCl₂–H₂O and the ρ can be obtained by formula (8) [30]:

$$Ba = \left[144.3 - \left(\frac{144.3}{\gamma} \right) \right] = \left[144.3 - \left(\frac{144.3}{\rho/1000} \right) \right] \quad (8)$$

where γ is the specific gravity.

When the Ba was measured, the ρ was calculated by Equation (5), and the P of the solution was obtained by comparing the solution density with the data in Table 4, obtained from a chemistry manual [31]. Equations (7) and (8) are also often used to calculate the ratio of MOC raw materials and the quantities of MOC materials. In the traditional preparation process for MOC, the relationship between brine and MgO can be calculated by Formulas (4)–(8) on the basis of obtaining the activity value of magnesium oxide and the molar ratio of MgO/MgCl₂, and Formulas (4)–(8) can be regarded as the traditional derivation of the mixture ratio of MOC, namely, the derivation of formula (DF).

Table 4. Standard data of the brine.

P^* (%)	ρ^* (kg/m ³)	Ba^* (°Be')	$Ba_i^* - C_i^*$
2	1014.6	2.1	0.1
4	1031.1	3.3	−0.7
6	1047.8	6.6	0.6
8	1064.6	8.8	0.8
10	1081.6	10.9	0.9
12	1098.9	13.0	1.0
14	1116.4	15.0	1.0
16	1132.4	16.8	0.8
18	1152.3	19.0	1.0
20	1170.6	21.1	1.1
25	1218.4	25.8	0.8
30	1268.8	30.6	0.6

* Standard data from manual.

The above DF may be complicated because the ρ needs to be calculated, and the P needs to be determined. Technicians hope to obtain the brine dosage directly and simply in practical engineering applications. In addition, the raw material bischofite used in MOC products is usually a byproduct of potassium extraction from salt lakes and contains certain impurities and other components (Table 1). As the standard mass concentration for $MgCl_2$ is defined using high-purity raw materials, in practical industrial applications, errors may occur when impure raw materials are used to define the standard. The error caused by this impurity leads to the deviation of the final dosage of bischofite or brine in practical applications.

3.2. Modification of Formula (MF)

Due to the large unit scale value of Ba and its easily accessible data, to accurately control the brine concentration and the dosage in MOC raw materials, the Ba is usually used to calculate the mass percentage concentration of the solution in industrial production. Therefore, to avoid the lengthy process and errors caused by the application of P , it is necessary to establish a connection between Ba and a in the scale production of MOC.

In Table 3, the P and Ba of the $MgCl_2-H_2O$ formed by the dissolution of bischofite from water at ambient temperature (20 °C) exhibited a linear growth trend, and the average difference between them was 0.9. The relationship between the Ba of bischofite in tap water and its P can be defined as

$$\text{Avg. } (Ba_i - P_i) = 0.9, (i = 1, 2, 3 \dots) \quad (9)$$

The data in Table 4 were from the standard manual [31]. In the standard data, the average $[Ba_i^* - P_i^*] = 0.7$, which deviates from the test data (Equation (9)) by 0.2. This deviation occurs because the bischofite in salt lake water contains some impurities, which affect the P of $MgCl_2-H_2O$. Based on the above tests, when bischofite is used as the liquid phase material of MOC, $(Ba - 0.9)$ can be directly used to replace P . Equation (9) was substituted into Equation (7) to obtain the MF applicable to the ratio of bischofite to the MOC material:

$$\frac{m_{Br}}{m_{MO}} = 2.375 \frac{a}{n (Ba - 0.9)} \quad (10)$$

After the simplification of the DF, the relationship between brine and MgO can be calculated by formula (10) on the premise of obtaining the magnesium oxide activity value and the molar ratio of $MgO/MgCl_2$; therefore, the Formula (10) is the modification of formula (MF).

3.3. Relationship between the Amount of Water in Brine and Bischofite

MgCl₂–H₂O of a certain concentration was formed after the bischofite solution was dissolved in water. The water in the solution comes from the crystal water in bischofite and the free water in dissolved bischofite; that is, the total amount of water (m_{HO}) was the sum of the crystal water (m_j) and free water (m_f), as shown in Equation (11).

$$m_j + m_f = m_{\text{HO}} \quad (11)$$

It can be seen from Equation (11) that MgCl₂–H₂O of different concentrations was formed after bischofite was dissolved in water, and the proportional relationship between the added m_f and the bischofite mass (m_{Bi}) can be expressed as follows:

$$\frac{m_f}{m_{\text{Bi}}} = \frac{m_{\text{HO}} - m_j}{m_{\text{Bi}}} \quad (12)$$

From the mass percentage concentration expression, the mass ratios of H₂O and MgCl₂ in MgCl₂–H₂O can be deduced:

$$P = \frac{m_{\text{MC}}}{m_{\text{MC}} + m_{\text{HO}}} \Rightarrow \frac{m_{\text{HO}}}{m_{\text{MC}}} = \frac{1}{P} - 1 \quad (13)$$

The relationship between the mass of water and MgCl₂ in solution and the Ba was obtained by substituting (9) into (13).

$$\frac{m_{\text{HO}}}{m_{\text{MC}}} = \frac{1}{(Ba - 0.9)/100} - 1 \quad (14)$$

The molecular weights of bischofite, MgCl₂, and 6H₂O are 203, 95 and 108, respectively; therefore, the masses of MgCl₂ and its m_j were, respectively,

$$m_{\text{Bi}} = m_{\text{MC}} \div \frac{95}{203} = 2.1368 m_{\text{MC}} \quad (15)$$

$$m_j = m_{\text{MC}} \div \frac{95}{203} \times \frac{108}{203} = 1.1368 m_{\text{MC}} \quad (16)$$

By substituting Equations (14)–(16) into Equation (12), the proportional relationship between m_f and the bischofite in the solution was obtained:

$$\frac{m_f}{m_{\text{Bi}}} = \frac{1}{0.021368 (Ba - 0.9)} - 1 \quad (17)$$

When bischofite was dissolved in water, MgCl₂–H₂O of a certain concentration was formed. The ratio of m_f added to the bischofite was a function of the Ba : $f(m_f/m_{\text{Bi}}) = f(Ba)$, which can be calculated according to Equation (17). As shown in Table 3, the actual measured function is expressed as $f(m_f/m_{\text{Bi}}) = f(Ba)$. As shown in Table 4, the Standard data is expressed as $f(m_f/m_{\text{Bi}})^*$. The calculated proportion and the actual proportion fitting curves are displayed in Figure 1. The fitting curves obtained by the two methods were approximate, and the calculated proportion fitting curve was slightly higher than the actual proportion fitting curve. This was mainly because in the actual measurement process, there may be some deviation in the fractional part of the Ba reading. For example, when $f(m_f/m_{\text{Bi}}) = 1.02$, the test Ba was 24.2 °Be', while the accuracy of 0.2 °Be' showed some deviation in the reading, resulting in a slightly higher computational proportion simulation curve.

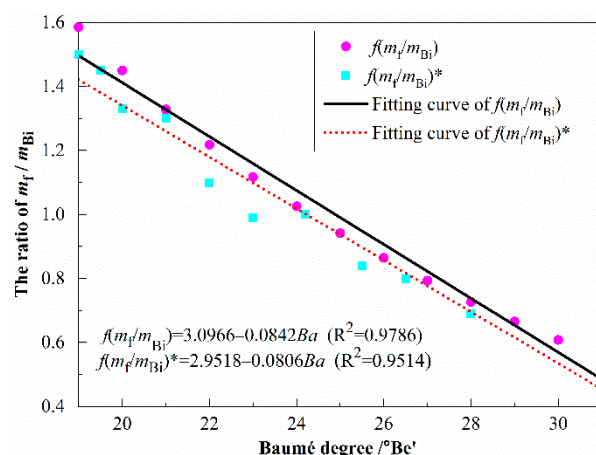


Figure 1. The ratio of free water to bischofite.

3.4. Water-to-Cement Ratio (W/C) with Caustic Dolomite MOC

Previous studies have proved that MOC products have the best performance when the optimal molar ratio of $MgO_a/MgCl_2$ approaches $n = 7$ [28,29]. At present, most manufacturers fix the raw material molar ratio at around 7. To maintain this constant, different concentrations of $MgCl_2-H_2O$ and dosage should be determined in tests or production according to the activity of magnesia powder. However, the active content and composition of industrial LMP usually change, and when CDP is added to LMP, the concentration and dosage of $MgCl_2-H_2O$ change again. Therefore, the best method was to analyze the brine consumption by CDP-MOC via quantitative analysis and variable analysis; that is, the total water consumption in MOC was divided into three parts: m_j , m_f and m_t . Among them, the m_t was the internal water of the bischofite. When bischofite was dissolved in water, the m_t also turned into a solvent and was used for the quantitative analysis. The m_f was the amount of water added to prepare bischofite at a certain concentration, and it changes with the brine concentration; thus, it was used for semiquantitative analysis. It reacts with m_f in the MOC system with MgO_a and $MgCl_2$ to form the 5·1·8 phase. The m_t plays a role in regulating the workability of MOC slurry, which is completely dependent on the composition of MgO ; the water was used for the variable analysis. Since the external water of MOC comprised m_f and m_t , the W/C of MOCFC can be expressed as

$$f\left(\frac{W}{C}\right) = \frac{m_f + m_t}{m_{MO}} \Rightarrow f\left(\frac{W}{C}\right) = \frac{m_f}{m_{MO}} + \frac{m_t}{m_{MO}} \quad (18)$$

Equation (17) was substituted into Equation (18) to obtain

$$f\left(\frac{W}{C}\right) = \left(\frac{1}{0.021368 (Ba - 0.9)} - 1\right) \frac{m_{Bi}}{m_{MO}} + \frac{m_t}{m_{MO}} \quad (19)$$

Since the mass of MgO consisted of CDP and LMP in the MOCFC system, the MgO_a was also divided into two parts: the MgO_a of CDP and the MgO_a of LMP. Let the MgO_a of CDP and LMP be a_1 and a_2 , respectively, and the mixing ratio of CDP and LMP be $x:y$; then, according to (10), the proportional relationship between the m_{Br} and m_{MO} in MOC with dolomite can be deduced as

$$\frac{m_{Br}}{m_{MO}} = 2.375 \frac{x a_1 + y a_2}{n P (x + y)} \quad (20)$$

Since the m_{MC} in $MgCl_2-H_2O$ was the product of the m_{Br} and P , Equations (14) and (20) were substituted into Equation (19) to obtain

$$f\left(\frac{W}{C}\right) = 5.0749 \left(\frac{1}{0.021368 (Ba - 0.9)} - 1\right) \frac{x a_1 + y a_2}{n (x + y)} + \frac{m_t}{m_{MO}} \quad (21)$$

It can be seen from Equation (21) that the W/C in the MOC was composed of two parts. The ratio of m_f to MgO was a function of Ba and MgO_a , and the ratio of m_t to MgO was a function of the volume of the m_t :

$$f\left(\frac{W}{C}\right) = f(Ba) + f(m_t) \quad (22)$$

3.5. Calculation Example

By means of the MF and brine relationship, the W/C relationship of LMP and CDP as MOC raw materials was obtained. Is this relationship feasible in the large-scale production of MOC? It also needs to be verified in actual production. As a result, ten groups of tests were used to verify the applicability of Equation (21), taking MOCFC as an example. The optimal molar ratio was set at 7 [7,24], the brine concentration was set at 25 °Be', and the foam volume added was 400 times the mass of MgO raw material according to the above analysis. Since it is easy to obtain MOCFC with excellent mechanical performance when $W/C = 0.5-0.6$, samples with different $x:y$ ratios at $W/C = 0.45-0.63$ were selected for intensity testing (as shown in Figure 2). The intensity of MOCFC with different $x:y$ ratios increased with W/C at the beginning and then decreased after reaching the peak. Generally speaking, within a suitable W/C range, the higher the content of MgO_a in the raw material is, the easier it is to obtain MOCFC with higher intensity. When the content of dolomite is relatively high, for example, $x:y = 5:1$, it is easier to obtain stable mechanical performance. When $W/C < 0.51$, given the high proportion of MgO_a in the raw materials and the low water content, the MOC slurry has a large amount of heat of hydration and undermixed powder, which makes it difficult to add foam into the slurry and impossible to shape the MOCFC. From the W/C mechanical performance test (Figure 2), it can be concluded that for MOCFC with CDP and LMP being the raw materials, MOCFC with the best performance can be obtained when $W/C = 0.45-0.63$.

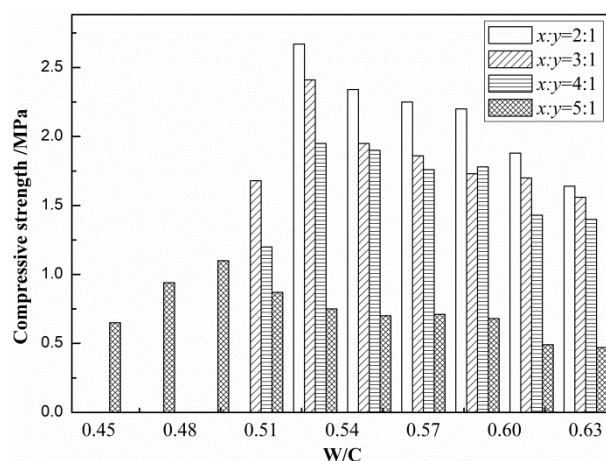


Figure 2. Compressive strength of magnesium oxychloride cement foam concrete (MOCFC) specimens cured in air.

According to Equation (21), the $f(Ba)$ at the mixing ratios of CDP and LMP of 2:1, 3:1, 4:1 and 5:1 can be calculated as 0.18, 0.16, 0.15 and 0.12, respectively. Since $f(Ba)$ is a fixed value calculated according to the formula, according to Equation (22), the mechanical performance of MOCFC changes with $f(m_t)$. As shown in Figure 3, the strengths of four MOCFC specimens with different mix ratios changed with a change in $f(m_t)$, and the $f(m_t)$ s of the specimens that reached the optimal strength were 0.35, 0.37, 0.38 and 0.37. According to Equation (21), the optimal W/C s for MOCFC were 0.53, 0.53, 0.52 and 0.49. The higher the MgO_a in the raw material for the MOC system, the greater the water consumption. The MgO_a among the four mixing ratios was of the following order: 2:1 > 3:1 > 4:1 > 5:1, which was consistent with the W/C trend obtained in the experiment.

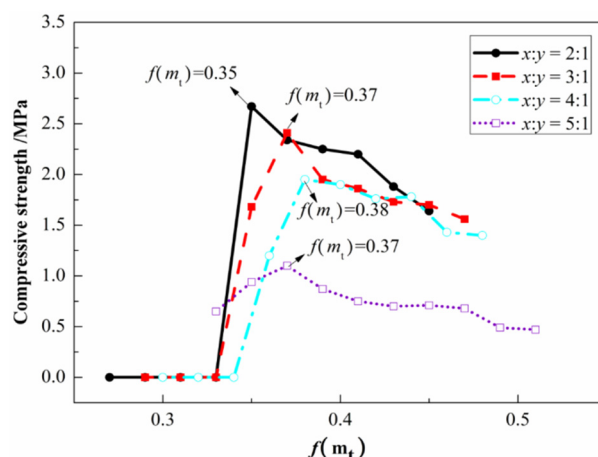


Figure 3. Compressive strength of MOCFC with different mix proportions on day 7.

The typical morphology of the $x:y = 2:1$ sample is shown in Figure 4. In the picture, the red arrows are pin-needle-like $5 \cdot 1 \cdot 8$ phase crystals [7,30], the blue arrows are $\text{Mg}(\text{OH})_2$ [32], and the purple arrows are bubble holes. The varied morphology of six types of MOCFC can be seen in the images. It is apparent that those in Figure 4a–c were covered with a thicker and larger $5 \cdot 1 \cdot 8$ phase in the bubble hole wall compared to those in Figure 4d–f. This contributed to the highest compressive strength of the controlled sample. When $f(m_t) = 0.35$, the bubble hole wall seems to have consisted entirely of $5 \cdot 1 \cdot 8$ phases. As $f(m_t)$ increased, the $5 \cdot 1 \cdot 8$ phase in the bubble wall gradually decreased, while the $\text{Mg}(\text{OH})_2$ gradually increased. This happened because with excessive water, the MgO_a generates more $\text{Mg}(\text{OH})_2$, which leads to a decrease in the intensity of the samples. We can see in Figure 4a that the walls of the bubble holes were covered by $5 \cdot 1 \cdot 8$ phase crystals, while in Figure 4b,c, it can be seen that small amounts of flake-like $\text{Mg}(\text{OH})_2$ began to occur, and in Figure 4e,f, it can be observed that $\text{Mg}(\text{OH})_2$ was so abundant that it also covered the bubble holes. The size of the $5 \cdot 1 \cdot 8$ phase showed the trend of $0.35 > 0.37 > 0.39 > 0.41 > 0.43 > 0.45$ in the bubble wall and the opposite trend in $\text{Mg}(\text{OH})_2$. A linear increasing relationship between the number of $5 \cdot 1 \cdot 8$ phase crystals and the proportion of W/C was shown, while $\text{Mg}(\text{OH})_2$ showed the opposite trend. Combining the results in Figure 2, when the W/C was increased from 0.51 to 0.63, the strength of the sample ($x:y = 2:1$) gradually decreased. $W/C = 0.54$ had the highest compressive strength (Figure 2); the corresponding $5 \cdot 1 \cdot 8$ phase crystals were the highest (Figure 4a), while when $W/C = 0.63$, the compressive strength was the lowest (Figure 2), and the corresponding $\text{Mg}(\text{OH})_2$ reached the highest (Figure 4e). The results observed from the SEM photo are consistent with those of the compressive strength test.

In previous work, it was suggested that the W/C of MOCFC with LMP ranged from 0.5 to 0.6, and the optimal test W/C was 0.55 [33,34]. These data are approximately equivalent to the findings in the current study, though the difference is that the activity of the doped CDP was less than that of the raw material; therefore, the W/C was less than 0.55, which also reflects the amount of brine and powder in the MOCFC of the real raw material. Combined with the actual preparation process for MOCFC, the “modification of formula” and the W/C relationship deduced above were feasible for the large-scale preparation of MOC using CDP and Salt Lake bischofite. The reason was that this model relationship shows the mechanical properties and corresponding microstructure initially involved in the above examples. The model relationship has the ability to truly reflect the material dosage relationship on the premise of ensuring the performance of MOC materials.

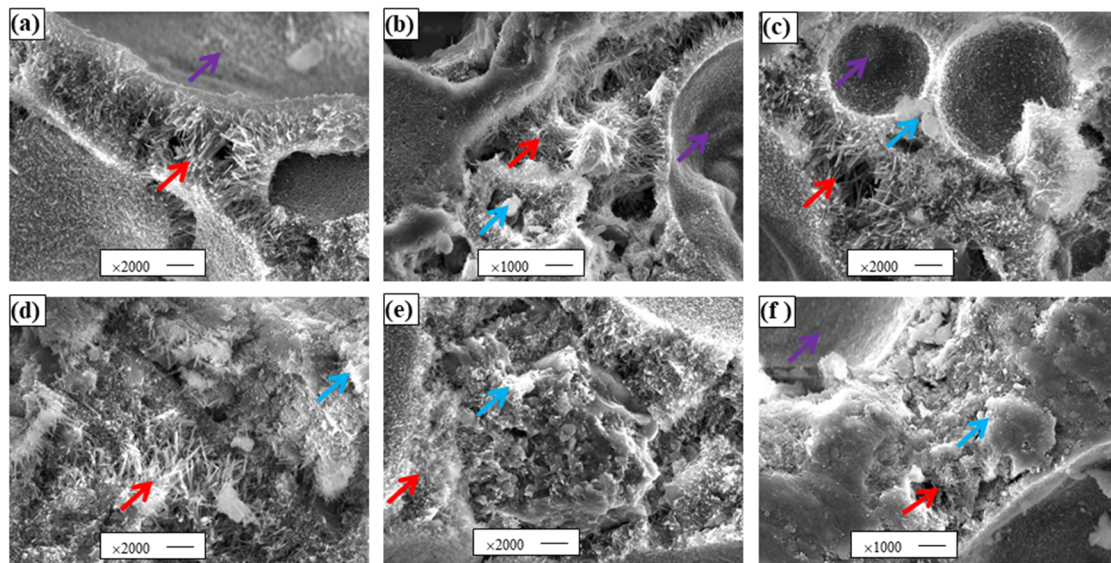


Figure 4. SEM images of MOCFC. (a–f) are samples of $f(m_t)$ equal to 0.35, 0.37, 0.39, 0.41, 0.43 and 0.45, respectively.

4. Conclusions

1. The physical properties of salt lake bischofite dissolved in water were first studied in this research. The P and Ba of $MgCl_2-H_2O$ formed by bischofite dissolved in water showed a linear growth trend at ambient temperature ($20\text{ }^\circ\text{C}$), and the average difference between the two was 0.9.
2. The ratio relationship between the m_{Br} and m_{MO} in MOC with dolomite was obtained using the mean difference ($\text{Avg.}(Ba_i - P_i = 0.9)$) and the MF: $m_{Br}/m_{MO} = 2.375 [(x a_1 + y a_2)/n P (x + y)]$. Then, the proportional relationship between the m_f added to bischofite was deduced, and the proportional relationship function was obtained: $f(m_f/m_{Bi}) = 1/0.021368 (Ba - 0.9) - 1$.
3. According to the MF, $f(m_{Br}/m_{MO})$ and the proportional relation function ($f(m_f/m_{Bi})$), the W/C relation formula for MOC with CDP was summarized: $f(W/C) = f(Ba) + f(m_t)$. It was verified through experiments that the W/C relationship of CDP–MOC can reflect the dosage relationship between the brine and powder in MOCFC under the conditions of real raw material ratios.
4. The derived MF formula and W/C relationship were verified in the practical production of MOCFC, and the optimum W/C range for MOCFC was obtained by using the W/C formula. It can be concluded that, for MOCFC with CDP and LMP being the raw materials, MOCFC with the best performance can be obtained when $W/C = 0.45\text{--}0.63$. The MgO_a among the four mixing ratios was of the following order: $2:1 > 3:1 > 4:1 > 5:1$, which was consistent with the W/C trend obtained in the experiment. As $f(m_t)$ increased, the 5·1·8 phase in the bubble wall gradually decreased, while the $Mg(OH)_2$ gradually increased. This happened because with excessive water, the MgO_a generates more $Mg(OH)_2$, which leads to a decrease in the intensity of the samples.

Author Contributions: All authors discussed and agreed upon the idea, and made scientific contributions: writing—original draft preparation, W.Z. and X.X.; experiment designing, J.W.; experiment performing, C.C. and S.A.; data analysis, W.Z.; writing—review and editing, W.Z. and J.D. All authors have read and agreed to the published version of the manuscript.

Funding: This research was funded by the Fund of Key Lab of Plateau Building and Eco-Community in Qinghai, China (2019-SL-001), and supported by the fund of Applied Basic Research Project of Qinghai Province, China (2021-ZJ-750, 2020-ZJ-746), and the High-End Innovative Talents Thousand Talents Plan of Qinghai Province, China.

Institutional Review Board Statement: Not applicable.

Informed Consent Statement: Not applicable.

Data Availability Statement: No new data were created or analyzed in this study. Data sharing is not applicable to this article.

Conflicts of Interest: The authors declare no conflict of interest.

References

- Huang, J.; Ge, S.; Wang, H.; Chen, R. Study on Preparation and Properties of Intrinsic Super-Hydrophobic Foamed Magnesium Oxychloride Cement Material. *Appl. Sci.* **2020**, *10*, 8134. [[CrossRef](#)]
- Zaleska, M.; Pavlikova, M.; Jankovsky, O.; Lojka, M.; Pivak, A.; Pavlik, Z. Experimental Analysis of MOC Composite with a Waste-Expanded Polypropylene-Based Aggregate. *Materials* **2018**, *11*, 931. [[CrossRef](#)]
- Zaleska, M.; Pavlikova, M.; Jankovsky, O.; Lojka, M.; Antoncik, F.; Pivak, A.; Pavlik, Z. Influence of Waste Plastic Aggregate and Water-Repellent Additive on the Properties of Lightweight Magnesium Oxychloride Cement Composite. *Appl. Sci.* **2019**, *9*, 5463. [[CrossRef](#)]
- Kastiukas, G.; Ruan, S.; Unluer, C.; Liang, S.; Zhou, X. Environmental Assessment of Magnesium Oxychloride Cement Samples: A Case Study in Europe. *Sustainability* **2019**, *11*, 6957. [[CrossRef](#)]
- Jin, S.; Li, K.; Li, J.; Chen, H. A Low-Cost, Formaldehyde-Free and High Flame Retardancy Wood Adhesive from Inorganic Adhesives: Properties and Performance. *Polymers* **2017**, *9*, 513. [[CrossRef](#)]
- Wang, L.; Chen, L.; Provis, J.L.; Tsang, D.C.W.; Poon, C.S. Accelerated carbonation of reactive MgO and Portland cement blends under flowing CO₂ gas. *Cem. Concr. Compos.* **2020**, *106*, 103489. [[CrossRef](#)]
- Zheng, W.; Xiao, X.; Chang, C.; Dong, J.; Wen, J.; Huang, Q.; Zhou, Y.; Li, Y. Characterizing properties of magnesium oxychloride-cement concrete pavement. *J. Cent. South Univ.* **2019**, *26*, 3410–3419. [[CrossRef](#)]
- Pivak, A.; Pavlikova, M.; Zaleska, M.; Lojka, M.; Jankovsky, O.; Pavlik, Z. Magnesium Oxychloride Cement Composites with Silica Filler and Coal Fly Ash Admixture. *Materials* **2020**, *13*, 2537. [[CrossRef](#)] [[PubMed](#)]
- Liska, M.; Al-Tabbaa, A. Performance of magnesia cements in pressed masonry units with natural aggregates: Production parameters optimisation. *Constr. Build. Mater.* **2008**, *22*, 1789–1797. [[CrossRef](#)]
- Luong, V.T.; Amal, R.; Scott, J.A.; Ehrenberger, S.; Tran, T. A comparison of carbon footprints of magnesium oxide and magnesium hydroxide produced from conventional processes. *J. Clean. Prod.* **2018**, *202*, 1035–1044. [[CrossRef](#)]
- Wang, Y.; Chen, X.; Zhang, S.; Yang, P. Recycling of Spent Pot Lining First Cut from Aluminum Smelters by Utilizing the Two-Step Decomposition Characteristics of Dolomite. *Materials* **2020**, *13*, 5283. [[CrossRef](#)]
- Srinivasan, S.; Dodson, D.; Charles, M.J.; Wallen, S.L.; Albarelli, G.; Kaushik, A.; Hickman, N.; Chaudhary, G.R.; Stefanakos, E.; Dhau, J. Energy Storage in Earth-Abundant Dolomite Minerals. *Appl. Sci.* **2020**, *10*, 6679. [[CrossRef](#)]
- Yu, J.; Qian, J.; Wang, F.; Qin, J.; Dai, X.; You, C.; Jia, X. Study of using dolomite ores as raw materials to produce magnesium phosphate cement. *Constr. Build. Mater.* **2020**, *253*, 119147. [[CrossRef](#)]
- Wang, F.; Zhu, X.; Liu, H.; Lei, S.; Huang, D. Influence of Superhydrophobic Coating on the Water Resistance of Foundry Dust/Magnesium Oxychloride Cement Composite. *Materials* **2020**, *13*, 3431. [[CrossRef](#)]
- Azimi, A.H. Experimental investigations on the physical and rheological characteristics of sand–foam mixtures. *J. Non-Newton. Fluid Mech.* **2015**, *221*, 28–39. [[CrossRef](#)]
- Altiner, M.; Yildirim, M. Influence of filler on the properties of magnesium oxychloride cement prepared from dolomite. *Emerg. Mater. Res.* **2017**, *6*, 417–421. [[CrossRef](#)]
- Chen, Y.J.; Wu, C.Y.; Yu, H.F.; Chen, W.H.; Chen, C.; Zhang, S.H.; Chen, F.Y. Study of using light-burned dolomite ores as raw material to produce magnesium oxysulfate cement. *Adv. Cem. Res.* **2018**, *30*, 437–450. [[CrossRef](#)]
- Ruan, S.Q.; Liu, J.W.; Yang, E.H.; Unluer, C. Performance and microstructure of calcined dolomite and reactive magnesia-based concrete samples. *J. Mater. Civ. Eng.* **2017**, *29*, 04017236. [[CrossRef](#)]
- Mironyuk, I.F.; Gun'ko, V.M.; Povazhnyak, M.O.; Zarko, V.I.; Chelyadin, V.M.; Leboda, R.; Skubiszewska-Zieba, J.; Janusz, W. Magnesia formed on calcination of Mg(OH)₂ prepared from natural bischofite. *Appl. Surf. Sci.* **2006**, *252*, 4071–4082. [[CrossRef](#)]
- Wang, X.; Miller, J.D.; Cheng, F.; Cheng, H. Potash flotation practice for carnallite resources in the Qinghai Province, PRC. *Miner. Eng.* **2014**, *66–68*, 33–39.
- Liu, X.; Zhong, M.; Chen, X.; Li, J.; He, L.; Zhao, Z. Enriching lithium and separating lithium to magnesium from sulfate type salt lake brine. *Hydrometallurgy* **2020**, *92*, 105247. [[CrossRef](#)]
- Sun, Y.; Wang, Q.; Wang, Y.; Yun, R.; Xiang, X. Recent advances in magnesium/lithium separation and lithium extraction technologies from salt lake brine. *Sep. Purif. Technol.* **2021**, *56*, 117807. [[CrossRef](#)]
- Jiříčková, A.; Lojka, M.; Lauermannová, A.M.; Antončík, F.; Sedmidubský, D.; Pavlíková, M.; Záleská, M.; Pavlík, Z.; Jankovský, O. Synthesis, Structure, and Thermal Stability of Magnesium Oxychloride 5Mg(OH)₂·MgCl₂·8H₂O. *Appl. Sci.* **2020**, *10*, 1683. [[CrossRef](#)]
- Lojka, M.; Jankovský, O.; Jiříčková, A.; Lauermannová, A.M.; Antončík, F.; Sedmidubský, D.; Pavlík, Z.; Pavlíková, M. Thermal Stability and Kinetics of Formation of Magnesium Oxychloride Phase 3Mg(OH)₂·MgCl₂·8H₂O. *Materials* **2020**, *13*, 767. [[CrossRef](#)] [[PubMed](#)]

25. Wang, L.; Luo, R.Y.; Zhang, W.; Jin, M.M.; Tang, S.W. Effects of Fineness and Content of Phosphorus Slag on Cement Hydration, Permeability, Pore Structure and Fractal Dimension of Concrete. *Fractals* **2021**. [[CrossRef](#)]
26. Wang, L.; Jin, M.M.; Guo, F.X.; Wang, Y.; Tang, S.W. Pore Structural and Fractal Analysis of the Influence of FLY ASH and Silica Fume on the Mechanical Property and Abrasion Resistance of Concrete. *Fractals* **2021**. [[CrossRef](#)]
27. Wang, L.; Guo, F.X.; Yang, H.M.; Wang, Y.; Tang, S.W. Comparison of FLY ASH, PVA Fiber, MgO and Shrinkage-reducing Admixture on the Frost Resistance of Face Slab Concrete via Pore Structural and Fractal Analysis. *Fractals* **2021**. [[CrossRef](#)]
28. Li, Z.; Chau, C.K. Influence of molar ratios on properties of magnesium oxychloride cement. *Adv. Cem. Res.* **2007**, *37*, 866–870. [[CrossRef](#)]
29. Wang, F.; Yang, L.; Guan, L.; Hu, S. Microstructure and properties of cement foams prepared by magnesium oxychloride cement. *J. Wuhan Univ. Technol.-Mater. Sci. Ed.* **2015**, *30*, 331–337. [[CrossRef](#)]
30. Zheng, W.; Xiao, X.; Wen, J.; Dong, J.; Chang, C.; Huang, Q.; Man, Y.; Zhou, Y. Application of a new computational method to calculate the mixture composition of magnesium oxychloride cement. *Ceramics-Silikáty* **2019**, *63*, 157–163. [[CrossRef](#)]
31. Liu, G.; Ma, L.; Liu, J. *Huaxue Huagong Wuxing Shuju Shouce*; Chemical Industry Press: Beijing, China, 2003; pp. 475, 485.
32. Li, Y.; Yu, H.; Zheng, L.; Wen, J.; Wu, C.; Tan, Y. Compressive strength of fly ash magnesium oxychloride cement containing granite wastes. *Constr. Build. Mater.* **2013**, *38*, 1–7. [[CrossRef](#)]
33. Dai, M.; Zhang, H. Study on magnesium oxychloride cement material with porous with orthogonal experiment. *Concrete* **2013**, *3*, 134–140.
34. Huang, T.; Yuan, Q.; Deng, D. The role of phosphoric acid in improving the strength of magnesium oxychloride cement pastes with large molar ratios of H₂O/MgCl₂. *Cem. Concr. Compos.* **2019**, *97*, 379–386. [[CrossRef](#)]